

Chapter 6

PRECLINICAL DEVELOPMENT OF PY-IM POLYAMIDES
AS THERAPEUTICS FOR MULTIPLE MYELOMA

This chapter is based on a collaborative project with Patrick J. Frost (UCLA, West Los Angeles Veteran Affairs Hospital). The text of this chapter was taken in part from a MERIT grant application submitted to West Los Angeles Veteran Affairs Hospital, written by Patrick J. Frost.

Multiple myeloma (MM) is an incurable disease of malignant plasma cells characterized by high rates of relapse, resistance to drug therapies, and, despite some recent advances in treatments, an overall median survival of just 5-6 years (1-3). It is unclear why this disease is so difficult to cure, but it has been hypothesized that physiologic characteristics of the bone marrow (BM) microenvironment confer critical growth and survival advantages that protect MM (4, 5). The BM is known to be hypoxic ($pO_2 \sim 10\text{-}30\text{mmHg}$) (6) compared to most tissues (85-150mmHg) and paradoxically, while oxygen stress can kill tumor cells (7), low pO_2 conditions also promote MM tumor progression (8), angiogenesis (9, 10), and resistance to chemotherapy (11, 12). These pro-survival effects are known to be regulated by an adaptive cellular response mediated by several oxygen-sensitive transcription factors, the most important of these being the hypoxia-inducible factors (HIFs) (for review see (13)). HIFs are composed of a constitutively expressed β -subunit (HIF1 β /ARNT) and inducible α -subunits (HIF1 α , 2 α , and 3 α) whose expression is generally dependent upon oxygen levels and is regulated by proteasome degradation (Fig. 6.1A). While the exact roles that these α -subunits play in regulating the hypoxic responses of MM in the BM microenvironment isn't well understood, recent studies do suggest that HIF1 α activity supports initial survival and angiogenesis, whilst HIF2 α supports subsequent MM progression and growth (3, 14). Thus, since the BM is known to have hypoxic niches that support MM growth and survival, and the adaptive cellular response to hypoxia includes

activation of HIF, we hypothesize that targeting this HIF-mediated adaptive hypoxic response will sensitize or kill MM cells engrafted within the BM microenvironment.

HIF activates about ~100-200 genes, typically in “categories” related to metabolism, angiogenesis, and apoptosis (15, 16). Because of the development of more resistant and malignant tumor phenotypes associated with hypoxia, there is increasing interest to targeting HIF-mediated gene transcription (17). Whilst targeting HIF-mediated transcription may be a promising strategy, there are numerous barriers to success. For example, many DNA targeting/binding molecules are non-specific and have significant “off target” effects against tumor and normal tissue (18). Echinomycin, a cyclic peptide in the family of quinoxaline antibiotics, can inhibit HIF/DNA binding (19), but is less sequence specific than HIF-PA (20). Programmable HIF inhibitors, such as siRNA or zinc-finger peptides, are sequence specific but suffer from poor bioavailability and the need for specific targeting strategies (21). Hairpin polyamides have an advantage for targeting gene transcription; they are small synthetic molecules, are cell permeable, localize to the nuclei, and can recognize and bind specific regions of the minor groove of double helical DNA with high affinity (22). The sequence specificity is conferred by the pattern of side-by-side pairs of Py and Im residues: Im-Py targets a G-C base pair, Py-Im targets a C-G base pair, and Py-Py targets T-A or A-T base pair (Fig. 6.1B) (23). Polyamide binding results in allosteric changes to the DNA helix that interferes with DNA-protein interactions and modifies endogenous gene expression (22). Specific PA compounds have been developed to recognize and target the promoter regions of enhancer and transcription factor binding elements, including androgen receptor (AR) (24), glucocorticoid receptor (GR) (25), NF-

κ B (26), and the TGF- β 1 promoter region (27). In xenograft studies, polyamides demonstrated anti-tumor efficacy related to their ability to inhibit specific gene expression, thereby providing a strong justification for further pre-clinical studies (28-32). Olenyuk et al (33) developed a PA that targets the 5'-WTWCGW-3' (W= A or T) sequence that modulates a subset of hypoxia-induced genes and confirmed that HIF/DNA targeting PA could be specific inhibitors of HIF activity (20).

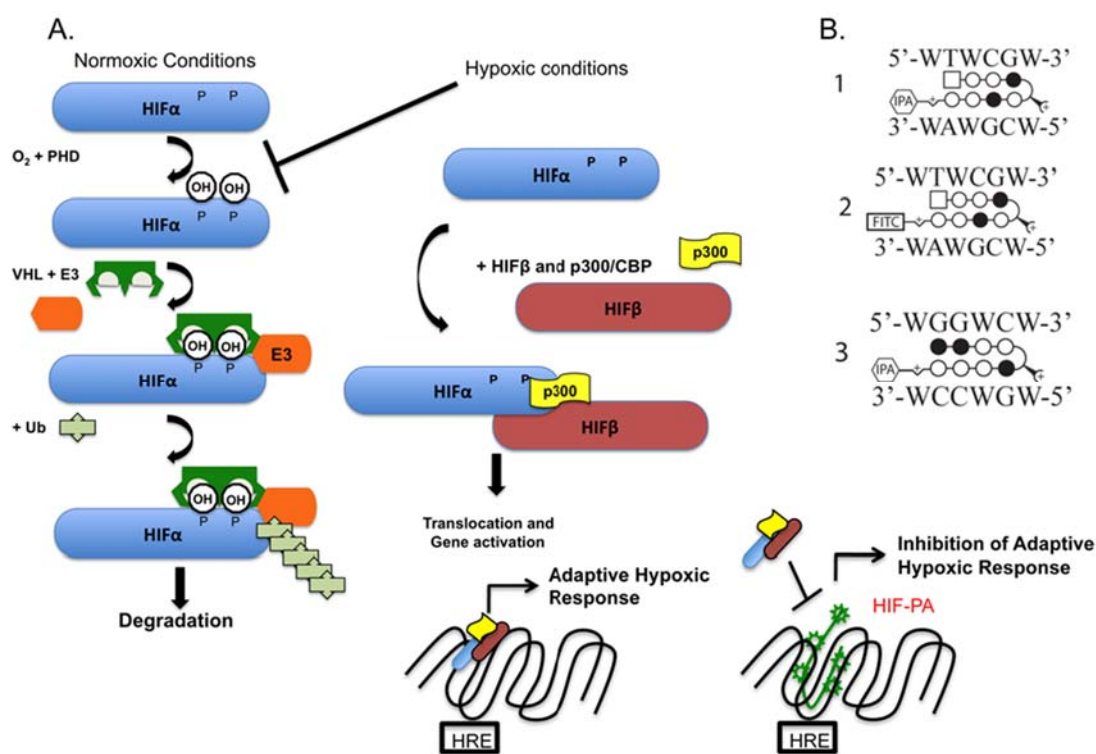


Fig 1: (A) Cartoon of HIF regulation showing O₂-dependent stabilization of HIF α and dimerization with HIF β . (B) Cartoon of PA used in this study (1) HIF-PA, (2) FITC-HIF-PA, (3) CO-PA.

This hypothesis was tested using a class of synthetically derived, sequence-specific DNA-binding pyrrole-imidazole (Py-Im) polyamide (PA) molecules that are composed of the aromatic rings of N-methylpyrrole and N-methylimidazole amino acids that recognize

the promoter regions of enhancer and transcription factor binding elements within DNA sequences (Fig. 6.1B) (33). The binding of Py-Im PA compounds results in allosteric changes to the DNA helix that interferes with DNA-protein interactions and modifies gene expression (22). These compounds have multiple advantages for targeting gene transcription: they are cell permeable, localize to the nuclei, and recognize and bind to specific regions of the minor groove of double helical DNA with affinity similar to transcriptional factors, such as HIF (22). Previous studies show antitumor effects of Py-Im polyamides in xenografts (20, 26, 28, 30); however, the effects of Py-Im polyamide treatment on Multiple Myeloma models have not been examined. Herein we evaluate those effects using a Py-Im polyamide (HIF-PA) that is capable of displacing heterodimer from binding to its cognate DNA sequences and inhibiting hypoxia-mediated gene transcription including pro-angiogenic factors (33). The choice of compound is dictated by observed heightened expression of angiogenic factors, such as VEGF, increased angiogenesis within MM tumors, and a strong correlation of these characteristics with disease development and progression in the BM and poor patient prognosis (34-37). Currently used VEGF-targeting drugs, such as bevacizumab (Avastin) inhibit angiogenesis in MM tumors; however, only modest and transient anti-tumor effects were observed (38), calling into question the overall clinical effectiveness of using a mono-therapeutic strategy targeting angiogenesis to treat myeloma. One explanation for the underwhelming effects of bevacizumab could be explained by a concomitant increase of hypoxia resulting from the inhibition of angiogenesis (39). In this scenario, low pO_2 (a natural component of the BM niche) may actually support MM progression and facilitate the adaptive hypoxic response via

activation HIF signaling and transcription of survival factors. In fact, a growing body of evidence supports the idea that HIF activity confers resistance to hypoxia-mediated apoptosis in solid tumors (40) and chemotherapy-mediated apoptosis in MM (12, 41). Thus, anti-angiogenesis strategies that don't address the HIF-mediated adaptive response to hypoxia may potentiate MM survival. Here, we present preliminary data demonstrating that synthetically derived PA compounds specifically inhibit the HIF-mediated adaptive hypoxic response in MM cells and overcome their resistance to hypoxia-mediated apoptosis. We investigated hypoxic signaling and HIF-PA response in a panel of MM cell lines (U266, H929, OPM-2, MM1.S, 8226) and the IL-6 dependent ANBL-6 isogenic MM cell line that has been transfected with mutated *N-RAS* or *K-RAS* (42). ANBL-6 is an interesting model because oncogenic mutations of *RAS* occur in 30-40% of MM patients and are associated with progressive disease, resistance to therapy, poor survival, and induction of HIF1 α (43, 44), which makes them a good candidate for targeting HIF activity. Another cell model used are isogenic U266 cells transfected with a constitutively activated AKT allele (45). The 8226 cells were used to establish subcutaneous and orthotopic (bone marrow) xenografts and showed potential anti-tumor effects of HIF-PA-mediated. Finally, our preliminary experiments silencing HIF1 α expression mirror our results of targeting HIF activity with polyamides, thereby validating our overall strategy. Our results showing differential expression and regulation of HIF α -subunits to low pO₂ highlights the importance of understanding the role that these transcriptional factors play in mediating the hypoxic response of MM engrafted in the BM.

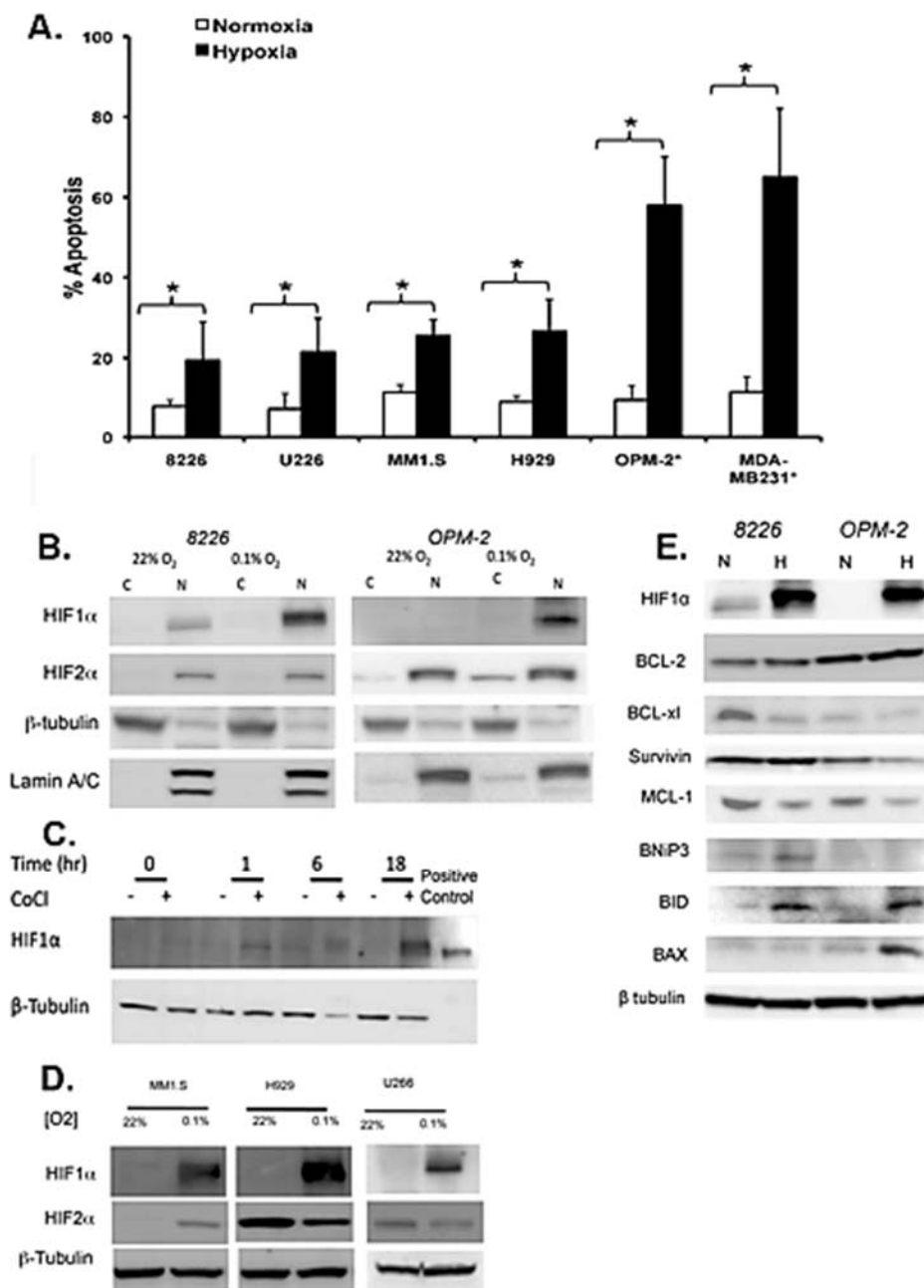


Fig 2. (A) Hypoxia-mediated apoptosis in MM cells cultured under normoxia (22%) or hypoxia (0.1%) for 72hr. Brackets indicate significance ($p < 0.05$). OPM2 and MDA-MB-231 cells were cultured at 0.1% O_2 for 48hr. Mean \pm Std dev of 4 independent experiments. (B) Immunoblots of HIF1 α and 2 α expression and translocation under normoxia or hypoxia for 24 hrs. C=cytoplasm fraction, N=nuclear fraction. (C) $CoCl_2$ induction of HIF1 α in OPM2. Lysates were collected at indicated times. (D) Immunoblots of hypoxia-mediated induction of HIF1 α and 2 α in MM cells. (E) Immunoblots showing effect of 24 hr hypoxia on anti- and pro-apoptotic factors in 8226 and OPM2 cells. N=normoxia (22%), H=hypoxia (0.1%).

Results

Regulation of hypoxic gene expression in polyamides

MM cell lines have been reported to be resistant to hypoxia (3), but variations in the pO₂ levels studied, use of hypoxia mimicking agents (i.e., CoCl₂) and variation in cell lines has introduced discrepancies between studies. To establish our own baseline model, we used a hypoxia chamber to test the sensitivity of MM cell lines cultured under standard “normoxic” conditions (i.e., ~22% O₂, 5% CO₂) or “hypoxic” conditions (from 2% down to 0.1% O₂). The O₂ levels (2-0.1%) we report here are similar to the actual pO₂ levels observed in mouse BM; Spencer et al (6) measured pO₂ in mouse bone marrow to be <32 mmHg, but in some BM niches it could be as low as 9.9 mmHg, or about 1% O₂ (range of 2-0.6%) in the extravascular spaces. We found that pO₂ levels >1% were only modestly cytotoxic to MM cells, even when cultured up to 72 hrs (data not shown). At low oxygen conditions (e.g., 0.5-0.1% O₂), we observed a statistically significant (T-test, p<0.05) increase in hypoxia-mediated apoptosis (Fig. 6.2A) with 8226 and U266 cells being the most resistant (an increase of ~15-20% apoptosis), whilst H929 and MM1.S were intermediately sensitive (~25% apoptosis). In contrast, OPM2 was the most sensitive (>50% apoptosis compared) and this affect occurred by 48 hr. As a positive control for hypoxia-mediated apoptosis, we used the breast cancer cell line, MDA-MB-231, which is known to be sensitive to low pO₂ (46). The hypoxia-resistant 8226 cells constitutively expressed HIF1 α , but this was strongly upregulated by hypoxia (0.1%, 24 hrs) (Fig. 6.2B left panel). HIF1 α was not observed in the hypoxia-sensitive OPM2 under normoxic

baseline conditions, but was induced by low pO₂ (Fig. 6.2B, right panel). Interestingly, HIF2 α expression was independent of O₂ levels in both cell lines. This is interesting because both

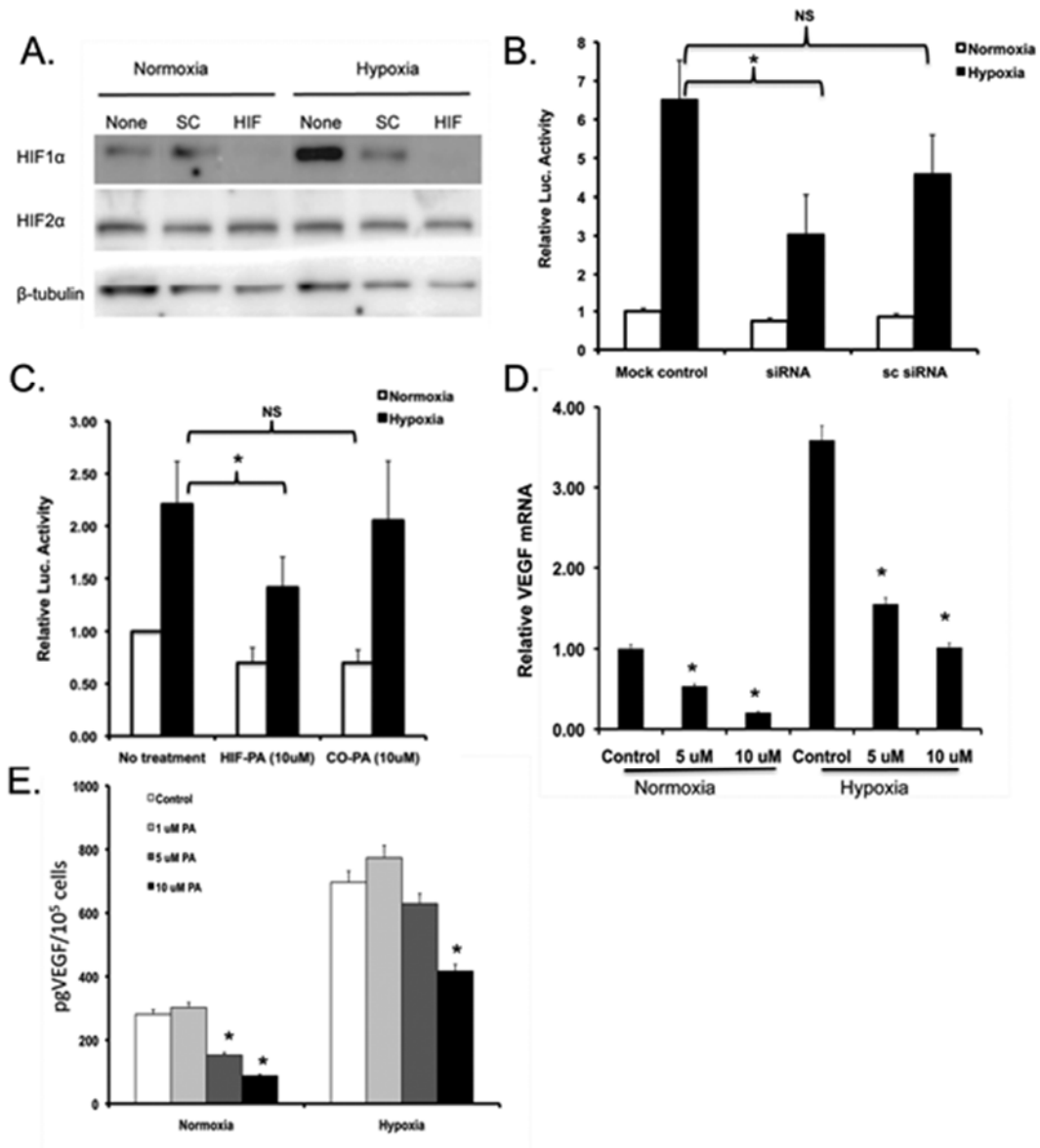


Fig. 6.3. (A) 8226 cells transfected with mock (None), HIF1 α siRNA (HIF) or scrambled siRNA (SC) and HIF1 α and HIF2 α measured by WB. (B). HRE-LUC reporter activity in 8226 cells transfected with HIF siRNA or SC siRNA as described above. Values are means \pm std of 3 independent experiments. NS=non significant ($p>0.05$), $*$ = $p<0.05$. Hypoxic conditions were set at 0.1% for 24hrs. (C) HRE-LUC activity in 8226 cells under normoxic or hypoxic conditions and

treated with PA as indicated above. (D) HIF-PA-mediated inhibition of VEGF mRNA by RT-PCR (*= $p < 0.05$). (E) HIF-PA-mediated inhibition of VEGF in supernatants by ELISA (*= $p < 0.05$).

α -subunits are controlled via the PHD/VHL ubiquitination pathway, yet it isn't clear why HIF2 α , but not HIF1 α , is constitutively expressed in these cells, and may lend credence to our hypothesis that the α -subunits have differential roles in MM. The rapid upregulation of HIF1 α in OPM2 was confirmed using the hypoxia mimic, CoCl₂, which induced HIF1 α by 1hr and reached a maximum by 18hrs (Fig. 6.2C). HIF1 α expression was also induced by low pO₂ in MM1S, H929, Mosby, and U266 cell lines (Fig. 6.2D). In contrast, MM1.S was the only cell line tested in which HIF2 α expression was O₂-dependent. These findings are generally similar to other reports describing HIF1 α expression in MM cells (3, 10, 14). Culturing 8226 and OPM2 with low oxygen (0.1% 24hrs) didn't affect the expression of the pro-survival factor Bcl-2, but did inhibit Bcl-xl and MCL-1 in OPM2 and 8226, whilst survivin was only downregulated in OPM2 cells (Fig. 6.2E). Survivin has previously been reported to play a role in HIF-regulated survival of myeloma cells and thus may be an important target for future studies (12). Low pO₂ also upregulated the pro-apoptotic factors, BNiP3 (a known HIF target), BID, and BAX. We wish to point out that it isn't clear if the changes described above are specifically due to HIF activation (and as such could be a target for HIF-PA) or represent general physiological stresses in cell caused by low pO₂.

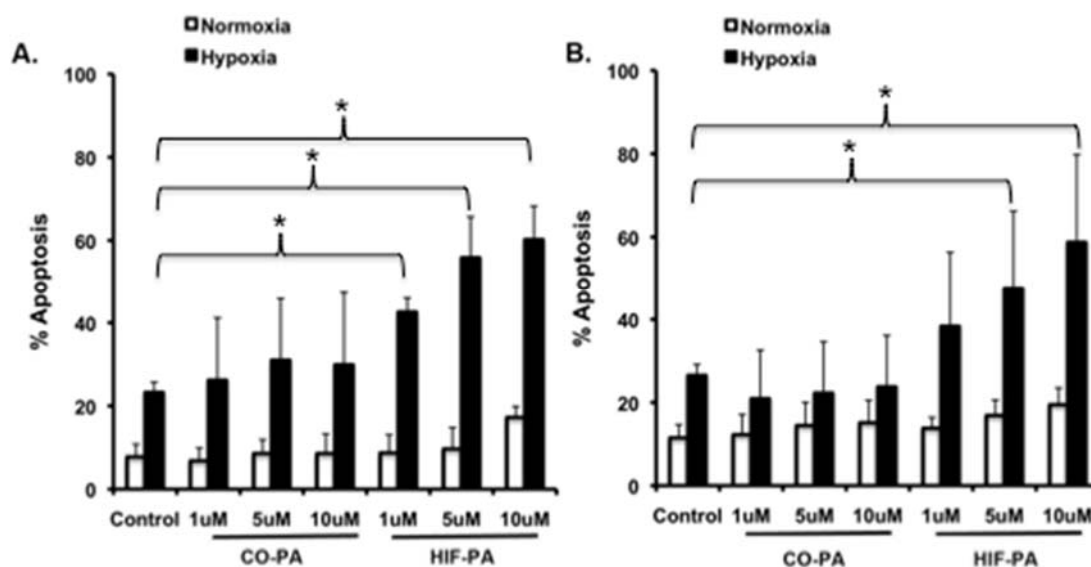


Fig. 6.4. HIP-PA sensitizes MM cells to hypoxia. (A) 8226 treated for 72 hr. (B) OPM2 treated for 24 hours. Apoptosis was measured by cleaved caspase 3. Cells were cultured under normoxic (22%O₂) or hypoxic conditions (0.1% O₂) with indicated concentration of HIF-PA or control PA. Data are means \pm SEM of 3 independent experiments. Brackets comparing control with treatment \ast = $p < 0.05$.

HIF-PA inhibits the hypoxic response in MM cells

HIF1 α siRNA was used to knockdown the baseline HIF1 α expression in 8226 cells (Fig. 6.3A), and importantly, this also inhibited the hypoxia-mediated upregulation of HIF1 α (Fig. 6.3A compare lanes 1 and 3 and 4 and 6) but not the expression of HIF2 α protein. Silencing HIF1 α with siRNA significantly inhibits HRE-LUC reporter activity in 8226 HRE-luciferase (HRE-LUC) transfected reporter cells (Fig. 6.3B). It should be noted that in these experiments, HIF1 α siRNA only inhibited about 50% of the HRE-LUC activity, which we believe is due to HIF2 α -mediated LUC activity, thus explaining the partial response we see. We also found that HIF-PA could inhibit the hypoxic response in 8226 reporter cells. As shown in Fig. 6.3C, hypoxic conditions (0.1% O₂, 24hr) induced (by ~2-3 fold) LUC activity compared to baseline and HIF-PA inhibited about 40-50% (4

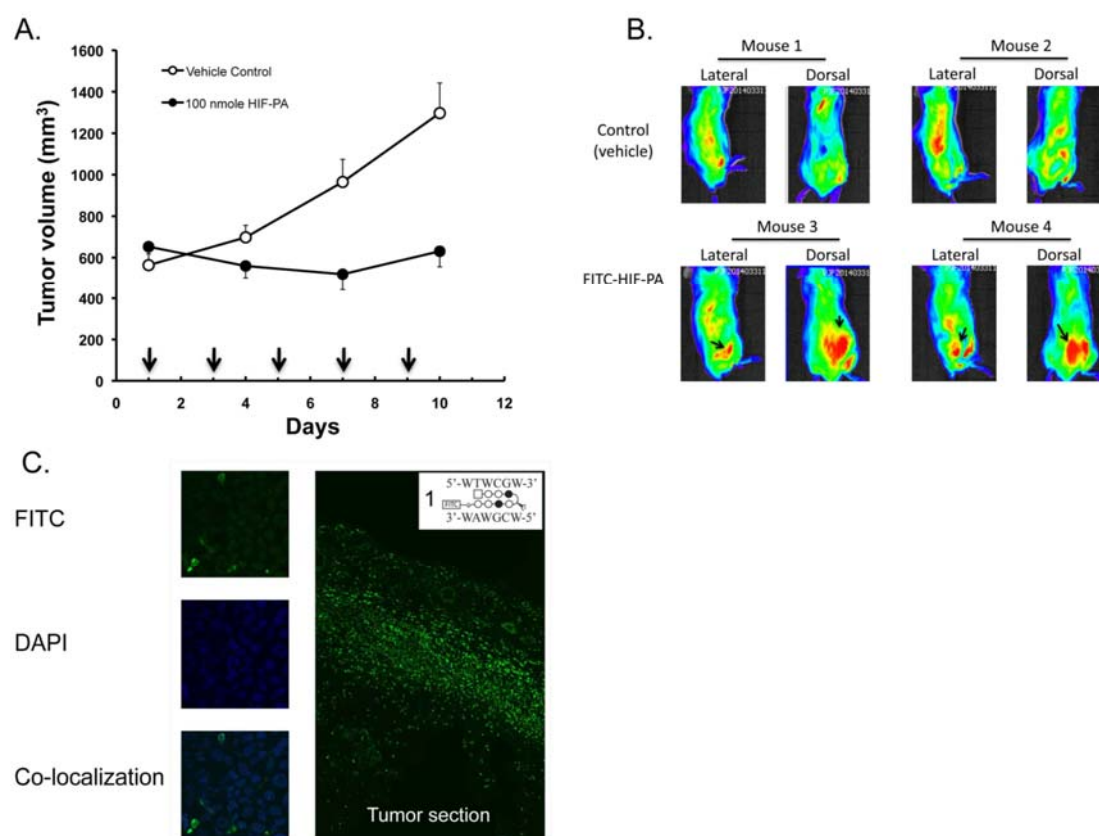


Fig 6.5. HIF-PA inhibits 8226 tumor growth in SQ xenograft model. (A) Change in 8226 tumor volume in HIF-PA treated NOD/SCID mice. Arrows indicate days of injection. * $p < 0.05$ (B) Uptake of FITC-labeled HIF-PA (3 injections, every other day) assayed using fluorescent imaging of live animals. Arrows indicate location of SQ 8226 tumors. (C) Confocal fluorescent microscopy of excised tumors, demonstrating nuclear uptake of HIF-PA.

independent experiments, $p < 0.05$) of this hypoxia-induced effect. As a negative control, non-HRE-sequence targeting CO-PA recognizing the unrelated sequence, 5'-WGGWCW-3', didn't significantly inhibit LUC activity. Similar results were seen in HRE-LUC expressing U266 and OPM2 cell lines (data not shown). In a previous study, it was shown that treatment with HIF-PA affected expression of a subset of hypoxia-induced genes containing HREs of the sequence 5'-(T/A)ACGTG-3' that was similar to the level of inhibition observed when HIF was silenced by siRNA and by the DNA binding drug,

Echinomycin (20). However, in this study, the effect of HIF-PA-mediated inhibition of gene expression was not studied for cells cultured under hypoxic conditions. To address this, we tested if VEGF gene transcription (a known target of HIF) was inhibited by HIF-PA in MM cells. As shown in Fig. 6.3D, culturing 8226 cells under hypoxic conditions (0.1% O₂, 24hrs) induced VEGF mRNA (by ~3-4 folds) and HIF-PA significantly (3 independent experiments p<0.05) inhibited this effect. Additionally, VEGF protein (measured by ELISA) in the supernatant of cells cultured in low pO₂ was also significantly downregulated (p<0.05)(Fig. 6.3E). Altogether, these data support the hypothesis that HIF-PA can inhibit the HIF-mediated adaptive hypoxic response in MM.

HIF-PA sensitizes MM to hypoxia

We expect that inhibiting the adaptive hypoxic response will sensitize MM cells to hypoxia-mediated apoptosis based on our preliminary data. To test this, we cultured MM cells under normoxic or hypoxic conditions (0.1% O₂, 72 hours) in the presence of HIF-PA or control. As shown in Fig. 6.4, HIF-PA had little effect on normoxic 8226 cells (Fig. 6.4 white bars), but HIF-PA treatment of hypoxic 8226 cells induced a significant and dose-dependent hypoxia-mediated killing (an increase in ~20% to ~60%)(ANOVA, P<0.05) (Fig. 6.4A left panel). OPM2 cell lines were even more sensitive to hypoxia and HIF-PA, (ANOVA, P<0.05) with similar increases in apoptosis being observed by only 24 hrs (Fig. 6.4B right panel). The control, CO-PA, had no effect on hypoxia-mediated apoptosis in either cell line. Similar results on hypoxia-mediated sensitization were seen with MM1S and U266 cells (data not shown). These data represent the results of 3 independent

experiments and support our hypothesis that inhibiting the adaptive hypoxic response with HIF-PA can overcome MM resistance to hypoxia-mediated apoptosis.

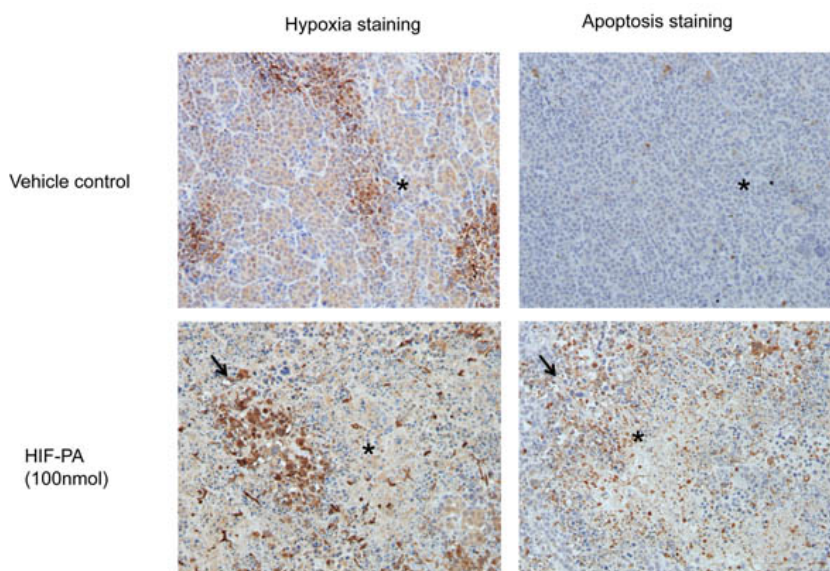


Fig. 6.6. Photomicrographs of serial tumor sections from control or HIF-PA treated mice stained for hypoxia (brown stain) and apoptosis (cleaved caspase 3). *=corresponding geographic regions. Arrow=areas of hypoxia and associated apoptosis.

As an *in vivo* correlate of the above data, the anti-MM effects of HIF-PA were also tested in a NOD/SCID xenograft model of subcutaneous (SQ) 8226 tumors (47-49). The mice were treated with 5 IP injections of HIF-PA (100nmol) or vehicle control every other day and the change in tumor volume was measured with calipers. HIF-PA treatment was well tolerated by the mice, with only a small transient decrease in weight. HIF-PA induced a significant inhibition of tumor growth in treated mice compared to control mice ($p < 0.05$) (Fig. 6.5A). In order to confirm uptake of HIF-PA, an additional group of mice (N=2 mice/group) were given FITC-conjugated HIF-PA to measure compound uptake by fluorescent imaging (Fig. 6.5B). There was some auto-fluorescence signal in the bladder

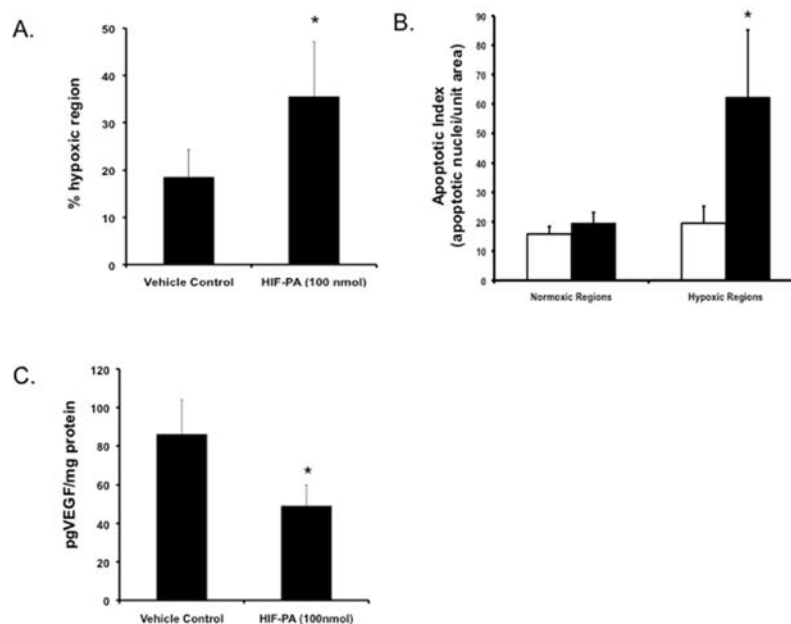


Fig 6.7. (A) Area of hypoxic regions in tissue sections stained for pimonidazole. (B). Apoptotic index, a measure of #apoptotic nuclei/unit area with regions of hypoxia or “normoxia”. (C) ELISA analysis of VEGF concentration in tumor lysate. * $P < 0.05$. Values are means \pm 95% CI.

and gut (Fig. 6.5B, mice #1 and #2) of control mice. However, in FITC-HIF-PA treated mice, a positive signal in the tumor nodules was noted (Fig. 6.5B see arrow in mouse #3 and #4) and was confirmed by fluorescent confocal microscopy of excised tumors (Fig. 6.5C). IHC for hypoxia and apoptosis of serial tumor sections is shown in Fig. 6.6 as described previously (49). Both control (top left panel) and HIF-PA (bottom left panel) treated tumors had regions of hypoxia (the brown stained areas), but the extent of hypoxia (as well as areas of necrosis) was greater in the HIF-PA treated tumors. Quantification of hypoxic regions (determined by area of positive staining) (10 tumors/group, 10 fields/tumor) was ~35% in nodules harvested from the HIF-PA treated mice, compared to about 18% in the tumors from mice treated with vehicle control ($p < 0.05$) (Fig. 6.7A). Necrotic regions within the HIF-PA treated tumors were greater than in control tumors,

and there was a strong physical correlation between areas of hypoxia and apoptosis (Fig. 6.6, bottom right panel), whilst apoptotic cells were evenly distributed in the control tumors (Fig. 6.6, top right panel). The apoptotic index (number of apoptotic cells/unit area) was used to quantify cell death by examining serial sections for hypoxic (determined by brown staining), and “normoxic” (determined by a lack of staining) regions and counting the number of apoptotic cells in the corresponding areas (10 tumors/group, 10 fields/region). As shown in Fig. 6.7B, there was an approximate 3-4 fold increase in apoptotic cells in the hypoxic regions of tumors from the HIF-PA treated mice compared to hypoxic regions of the control tumors ($p < 0.05$). HIF-PA also significantly inhibited VEGF expression in tumor lysate by ~50% when compared to control tumors (Fig. 6.7C). Our data supports the hypothesis that HIF-PA can target VEGF and angiogenesis *in vivo* but we don't think that inhibition of VEGF-mediated inhibition of angiogenesis is the only explanation for these results. For example, HIF-PA sensitized MM cells to hypoxia-mediated apoptosis *in vitro*, a situation in which VEGF and angiogenesis is likely not important to MM survival.

Anti-tumor effects of HIF-PA against MM engrafted in the BM.

We've developed an orthotopic, “disseminated” BM-engrafted model (based on that of Miyakawa (50, 51)) using LUC2-transfected 8226 cells that will allow us to study MM engrafted in the BM. As shown in Fig. 6.8A, NOG mice challenged with 8226LUC cells developed engrafted tumors determined by using bioluminescence and X-ray analysis (Fig. 6.8A). In these mice, 20-50% of the bone marrow cells from inoculated mice were positive for human CD45 as confirmed by flow cytometry using FITC-conjugated anti-huCD45

antibody (Fig. 6.8B) and by IHC of *in situ* CD45+ 8226 cells in the mouse femurs.

Gross histological analysis of the mice didn't show tumor formation in other tissues (i.e., liver, lung, spleen, or kidney). Other MM cell lines (e.g., OPM2, U266, and H929) are currently being developed and tested using this model.

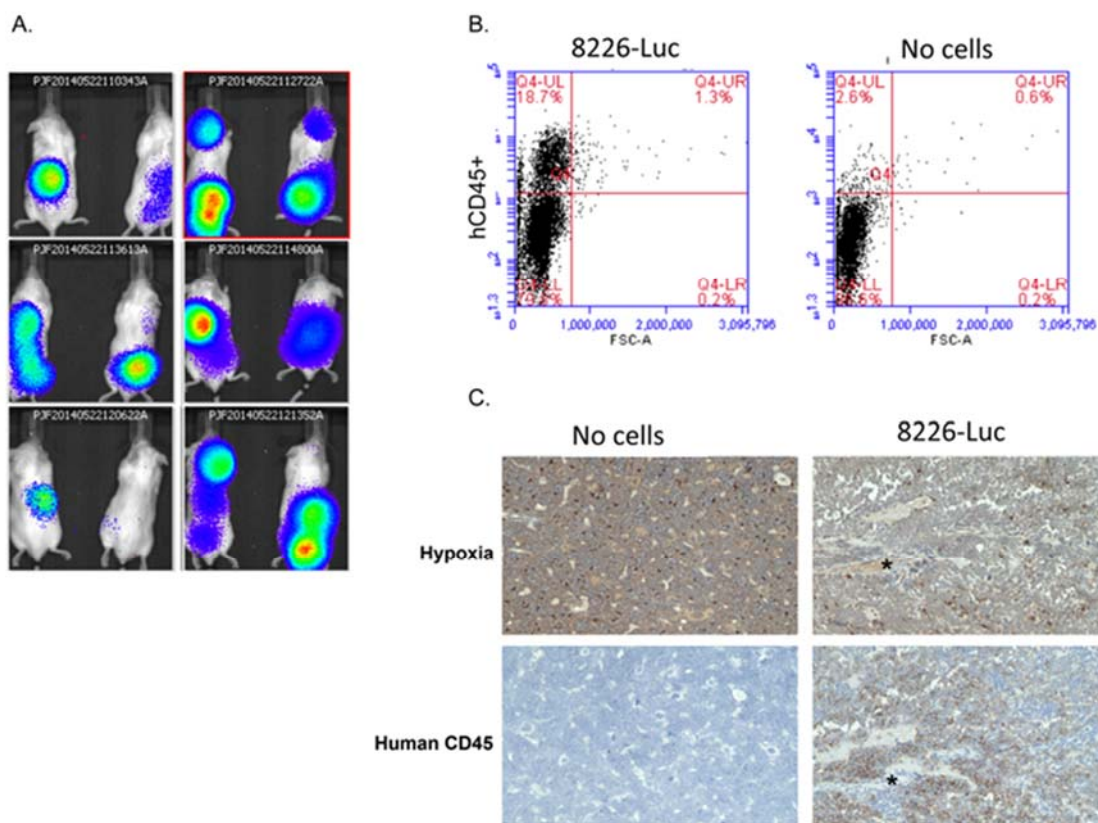


Fig 6.8. NOG mice challenged IV with 8226-LUC expressing cells. (A) Imaging of 12 mice on day +20 post-challenge with 8226LUC showing positive signal associated with long bones, skull, and spine. (B) BM harvested from mice challenged with 8226LUC or PBS and stained for huCD45 antibody (C). IHC of femurs of mice challenged with 8226LUC or PBS. Serial sections were stained with pimonidazole or huCD45.

Next, we performed a pilot experiment in which NOG mice (N=8 mice/group) with BM engrafted 8226LUC cells were given HIF-PA or vehicle control as described above for our SQ model. Fig. 6.9A shows that there was no significant (ANOVA, $p < 0.10$) inhibition of

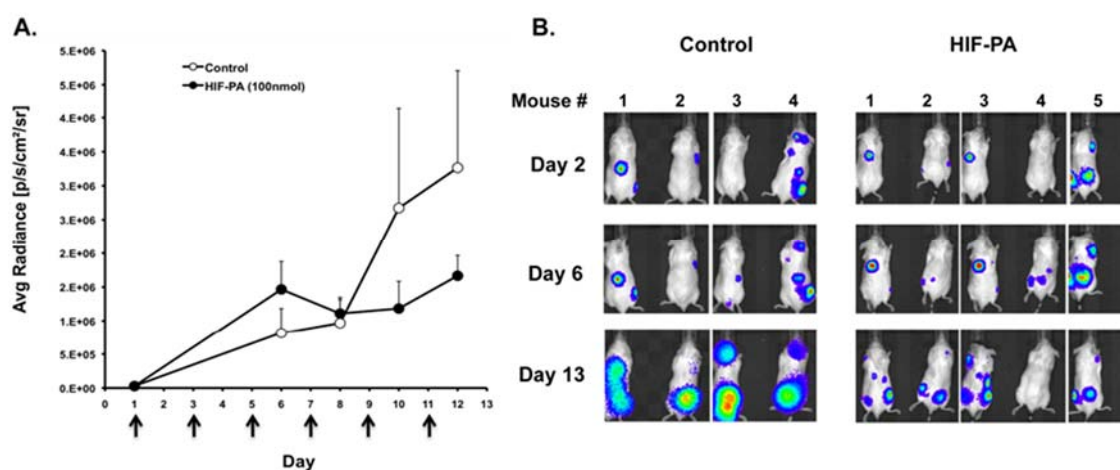


Fig 6.9. HIF-PA inhibits 8226 tumor growth in BM. (A). NOG (8/group) were challenged IV with 8226-LUC cells. Animals were given 5 IP injections of HIFA (100nmol) or vehicle control (arrows indicate days of injection). Luciferin bioluminescence was measured and data is presented as average radiance \pm 95% CI. * $p < 0.10$. (B) Representative pictures of mice imaged on day 2, day 6, and day 13 in control and HIF-PA treated mice showing change in Luciferin activity.

tumor growth in the BM and that increasing sample size will be required. Lack of significance was probably due to the small N and large variations in bioluminescence signal in the control mice. Representative images taken on day +2, +6 and +13 show both a decrease in LUC activity as well as a general shrinkage of individual tumor foci in the HIF-PA treated mice (Fig. 6.9B). In fact, we noted that in control mice, the tumor foci tended to grow and merge during the course of the experiment, in contrast to HIF-PA treated mice, in which the foci remain relatively small and isolated. This suggests to us that HIF-PA may inhibit both tumor growth and migration within the skeleton, suggesting further experiments to test this hypothesis.

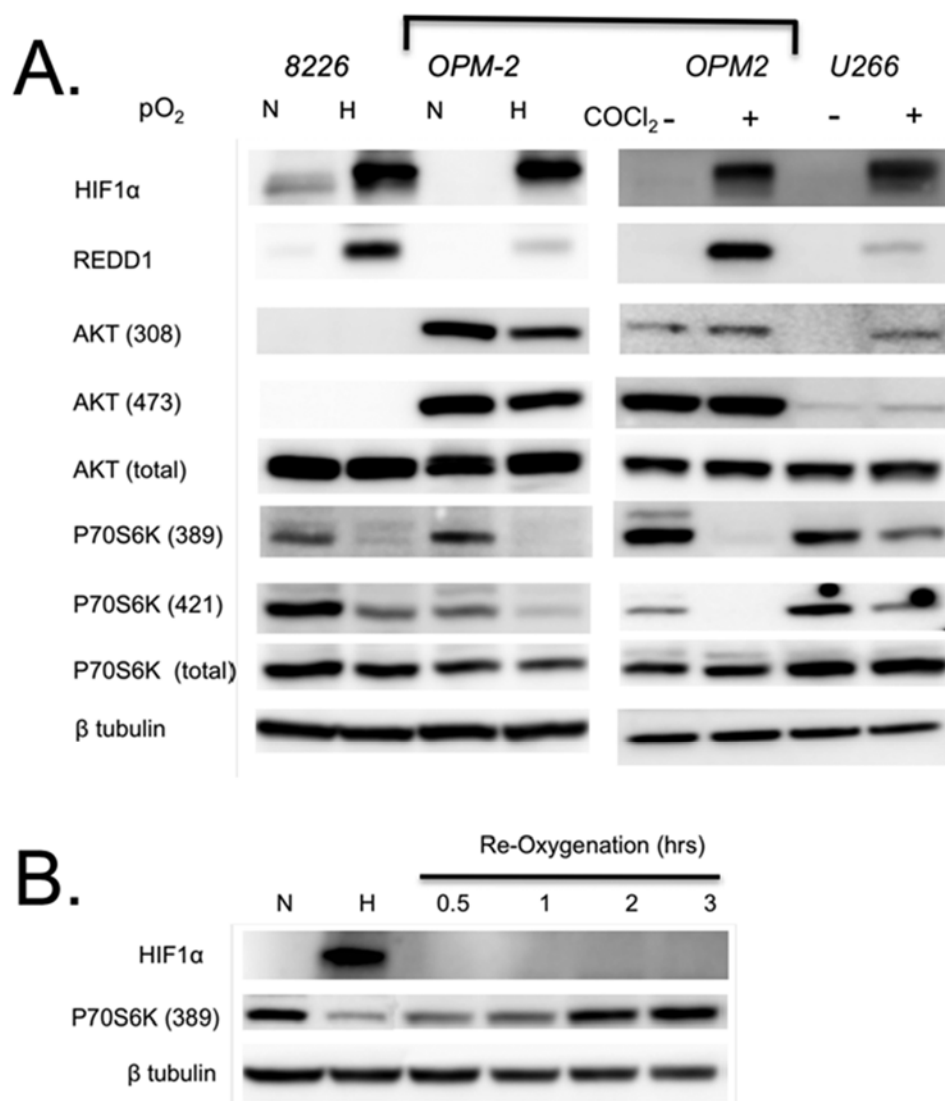


Fig 6.10. (A) Differential sensitivity of AKT/mTOR pathway in MM cells to 24hr hypoxia (0.1%) or CoCl₂ (100μM) treatment. Bracket indicates OPM2 treated with either hypoxia or CoCl₂. (B) OPM2 cells were cultured under normoxic or hypoxic (0.1%) conditions for 24 hrs and then allowed to re-oxygenate under normoxic culturing conditions for indicated time periods.

Effects of AKT/mTOR pathway activation on regulation of HIF-PA sensitivity: We have previously demonstrated that sensitivity of MM cells to mTOR inhibitors was correlated to heightened AKT activity *in vivo* and this was correlated with the inhibition of VEGF and angiogenesis (45, 47-49). Based on that we initially hypothesized that simply the induction of hypoxic stress could kill MM cells. However, as shown in Fig. 6.2, oxygen stress alone doesn't explain our *in vivo* observations, as MM tend to be resistant to low pO₂. In fact, MM cells that are most resistant to mTOR inhibition (and are characterized by quiescent AKT) also tend to be the most resistant to hypoxia (ie., 8226 and U266), whilst cells with hyperactive AKT tended to be the most sensitive (i.e., OPM2) (52).

One potential mechanism is that hypoxia induces REDD1 expression, a hypoxia-sensitive inhibitor of mTOR (53). Therefore, we asked what were the effects of hypoxia on the mTOR pathway in our model. As shown in Fig. 6.10, hypoxia (or treatment with the hypoxia mimic CoCl₂) induces REDD1 expression and inhibits the phosphorylation of p70S6 kinase, a downstream target of mTOR (54) (Fig. 6.10A). Hypoxia mediated inhibition of p70 was transient, returning to normal within 2 hr following reoxygenation of the cells (Fig. 6.10B). On the other hand, hypoxia has only slight effects on AKT phosphorylation in 8226 and OPM2 cells and actually increases AKT phosphorylation at T308 in U266 cells. There is also evidence that IGF-1 and IL-6-mediated signaling via AKT induces HIF activity and potentiates survival in MM cells (12). Finally, mutations in PTEN (tumor suppressor gene that regulates AKT) leads to increase HIF activity (55). Therefore, based on this and our previous work, we will test if sensitivity to HIF-PA is regulated by the activation of AKT/mTOR pathway in MM cells. To achieve this, we'll

use isogenic U266 cells that express a constitutively active AKT allele (45) as well as in ANBL-6 cells. The effects of HIF will be validated using our knockdown cells as described above. Specifically, we'll test if sensitivity to HIF-PA is correlated to AKT/mTOR activity.

In recent studies, it was shown that the hypoxia confers resistance to melphalan- or bortezomib-mediated apoptosis in MM cells, and silencing HIF1 α expression restored sensitivity (12, 41). However, targeting HIF using siRNA may not be clinically feasible approach, and may be limited due to its failure to target HIF2 α . Therefore, we would argue that abrogating HIF's ability to bind to the HRE using HIF-PA is a more effective way to overcome chemoresistance in MM. To test this hypothesis, MM cell lines and patient samples will be cultured *in vitro* under normoxic or hypoxic conditions and treated with HIF-PA in combination with bortezomib, melphalan, or mTOR inhibitors. These drugs were selected because they are either currently utilized anti-MM therapies (bortezomib and melphalan) or have been implicated in hypoxia-mediated apoptosis (mTOR inhibitors) in MM. In initial experiments, we'll measure the viability (by MTT assay), cell cycle transit (by hypotonic PI), and induction of apoptosis (using a cleaved caspase-3 assay kit) at various time points. We'll also collect RNA and protein to study the effects combination therapy on gene expression. The evaluation of drug-drug and drug-hypoxia interactions will be determined by isobologram and combination index (CI) analysis as previously described in our recently published study (56).

Our past studies have established that 8226 cells are resistant to mTOR inhibitors due, at least in part, to AKT dependent regulation of the internal ribosome entry site (IRES)-

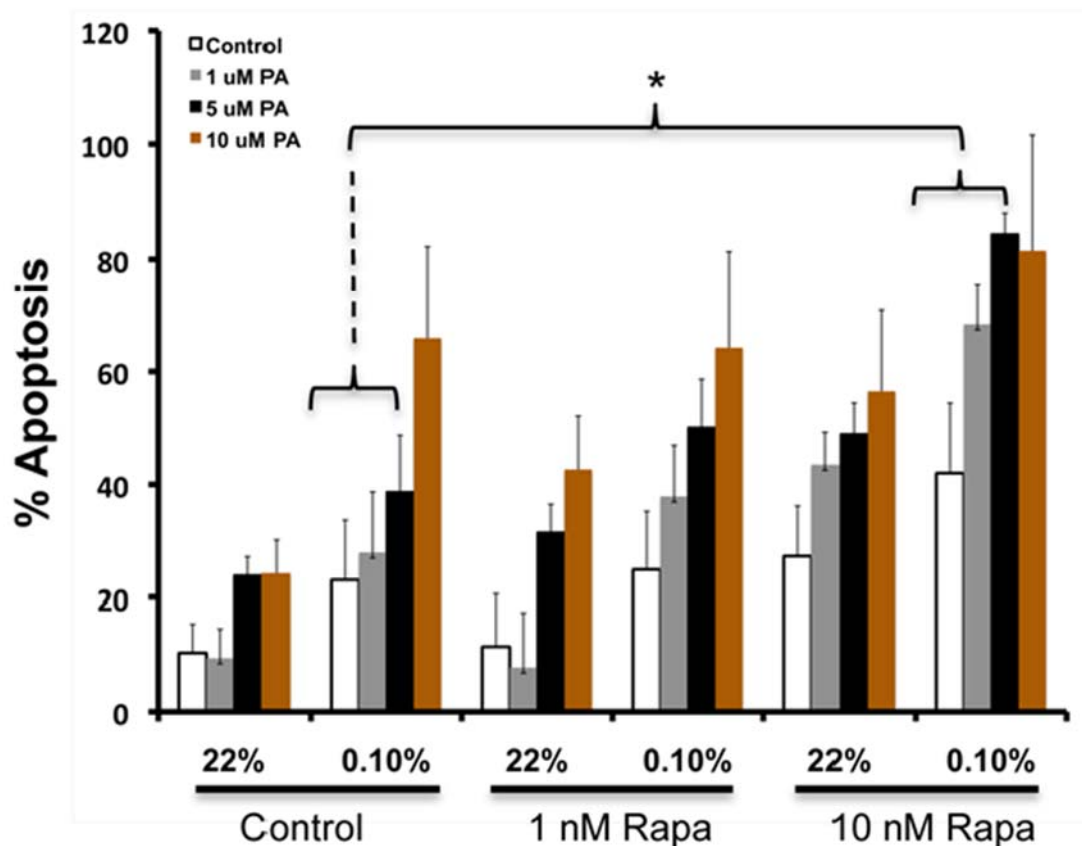


Fig 6.11. Combination of HIF-PA and Rapa treatment overcome resistance to hypoxia-mediated apoptosis. Cells were cultured under normoxic or hypoxic (0.1%) conditions with indicated drugs for 72hr. Values are mean \pm SEM of 3 independent experiments. Brackets and * indicates * $p < 0.05$.

mediated cap-independent salvage pathway that allows for translation of critical RNA species in the face of mTOR inhibition by rapalogs (i.e., rapamycin (RAPA) and temsirolimus) (45, 48, 49, 57, 58). We also demonstrated a correlation between RAPA-mediated inhibition of VEGF expression and angiogenesis with the induction of apoptosis in MM tumors *in vivo* (47, 48). Since hypoxia inhibits the mTOR pathway (53, 59, 60) and cap-dependent translation (61), this suggests a role of IRES activity in regulating MM

sensitivity to hypoxia (62). However, as shown in Fig. 6.2A, hypoxia alone isn't sufficient to kill 8226 MM cells. Therefore, we tested whether or not inhibiting mTOR-mediated translation could overcome resistance to hypoxia, the rationale being that inhibition of protein translation induced by the hypoxic response could sensitize the cells to apoptosis. Surprisingly, we found that mTOR inhibition had only a modest effect on apoptosis in MM cells cultured under hypoxic (0.1% O₂) conditions (Fig. 6.11, see white bars). However, the RAPA-resistant cell line, 8226, demonstrated a significant and synergistic HIF-PA-mediated sensitization to apoptosis in combination with RAPA, suggesting that targeting both the transcription and translation of hypoxia-induced genes would be an effective anti-MM strategy (Fig. 6.11, see grey and black bars and bracketed area). To expand on these findings, we'll study combination treatment of HIF-PA and mTOR inhibitors, including members of the rapalog family (e.g. rapamcyin, temsirolimus) that inhibit the mTOR complex 1 (mTORC1) and the new family of mTOR complex 1 and complex 2 (mTORC1/2) inhibitors (e.g., PP242) (63). Finally, we'll also study combination therapy of HIF-PA with bortezomib (a proteasome inhibitor) and melphalan (a nitrogen mustard alkylating agent) that were selected because they represent standard therapies for MM. As stated above, very interesting data has been presented indicating that hypoxia can confer resistance to these drugs in MM. Since these therapeutics are standard for treating MM, we believe that determining if HIF-PA can overcome MM resistance is clinically relevant and will be a major goal of this AIM.

Data and Statistical Analysis: All data collected will be compiled and maintained using the computer program Excel. Initial data exploration and analysis of all variables will be performed using summary tables (mean, standard deviation, and ranges) box plots, and line graphs. The null hypothesis (that there is no difference from the control) will be tested using one-way analysis of variance (ANOVA), Student *t*-tests, multiple linear regression models, and *post hoc* Tukey-Kramer pair-wise comparisons. A P-value < 0.05 will be considered statistically significant for rejecting the null hypothesis. The PI has access the UCLA Semel Institute Statistics Core that will provide expert guidance and consultation in the design and analysis of experiments with the appropriate level of statistical power.

Power analysis for mouse studies: A power analysis predicts 95% power to detect differences of 30% or greater in changes in our primary variable (tumor volume) using a sample size of 8 mice/group. The effect size for changes in tumor volume in drug-treated mice compared to controls was estimated from our preliminary data and previous studies to be between 30-50%. However, only approximately 75-100% of mice challenged with tumor cells (depending upon cell line) develop a SQ or BM engrafted tumors. Thus, to ensure 8 mice/group, a total of 10-16 mice will be injected with tumor cells per experiment. Overall, we expect to utilize about 200 mice/year.

Power analysis for patient samples: We assumed that the ED50 for HIF-PA-mediated cytotoxicity will be a continual variable under hypoxic conditions and dichotomized samples into high (i.e. constitutive expression) or low (no expression) for HIF1 α protein

examples. We also assumed that 33% of patient samples express “high” HIF1 α based on previous literature (9). Thus, we estimate we’ll need 25 patients to have 80% power and detect at least a 2x fold difference in the ED50 at a significance level of $\alpha=0.05$ (calculated by a 2 sided *t*-test). In consultation with Dr. Lichtenstein, we anticipate recruiting ~7-10 patient samples/year, which should allow us to complete these studies in the time frame of this MERIT. We are cognizant of the fact that patient history (such as newly diagnosed versus relapsed disease) will contribute to the variability of our model, but would argue that addressing these variables are outside the initial scope of this application. However, if our pre-clinical results are promising, we will expand our experimental design to incorporate these additional factors.

References

1. Kumar SK, *et al.* (2008) Improved survival in multiple myeloma and the impact of novel therapies. *Blood* 111(5):2516-2520.
2. Lonial S, Mitsiades CS, & Richardson PG (2011) Treatment options for relapsed and refractory multiple myeloma. *Clin Cancer Res* 17(6):1264-1277.
3. Martin SK, Diamond P, Gronthos S, Peet DJ, & Zannettino AC (2011) The emerging role of hypoxia, HIF-1 and HIF-2 in multiple myeloma. *Leukemia* 25(10):1533-1542.
4. Hideshima T, *et al.* (2001) Novel therapies targeting the myeloma cell and its bone marrow microenvironment. *Semin Oncol* 28(6):607-612.
5. Podar K, Chauhan D, & Anderson KC (2009) Bone marrow microenvironment and the identification of new targets for myeloma therapy. *Leukemia* 23(1):10-24.
6. Spencer JA, *et al.* (2014) Direct measurement of local oxygen concentration in the bone marrow of live animals. *Nature* 508(7495):269-273.
7. Hockel M & Vaupel P (2001) Biological consequences of tumor hypoxia. *Semin Oncol* 28(2 Suppl 8):36-41.
8. Asosingh K, *et al.* (2005) Role of the hypoxic bone marrow microenvironment in 5T2MM murine myeloma tumor progression. *Haematologica* 90(6):810-817.
9. Giatromanolaki A, *et al.* (2010) Hypoxia and activated VEGF/receptor pathway in multiple myeloma. *Anticancer Res* 30(7):2831-2836.
10. Storti P, *et al.* (2013) Hypoxia-inducible factor (HIF)-1alpha suppression in myeloma cells blocks tumoral growth in vivo inhibiting angiogenesis and bone destruction. *Leukemia* 27(8):1697-1706.
11. Hu J, *et al.* (2010) Targeting the multiple myeloma hypoxic niche with TH-302, a hypoxia-activated prodrug. *Blood* 116(9):1524-1527.
12. Hu Y, *et al.* (2009) Inhibition of hypoxia-inducible factor-1 function enhances the sensitivity of multiple myeloma cells to melphalan. *Mol Cancer Ther* 8(8):2329-2338.
13. Greer SN, Metcalf JL, Wang Y, & Ohh M (2012) The updated biology of hypoxia-inducible factor. *Embo J* 31(11):2448-2460.
14. Martin SK, *et al.* (2010) Hypoxia-inducible factor-2 is a novel regulator of aberrant CXCL12 expression in multiple myeloma plasma cells. *Haematologica* 95(5):776-784.
15. Pouyssegur J, Dayan F, & Mazure NM (2006) Hypoxia signalling in cancer and approaches to enforce tumour regression. *Nature* 441(7092):437-443.
16. Semenza GL (2011) Oxygen sensing, homeostasis, and disease. *N Engl J Med* 365(6):537-547.
17. Podar K & Anderson KC (2010) A therapeutic role for targeting c-Myc/Hif-1-dependent signaling pathways. *Cell Cycle* 9(9):1722-1728.
18. Gilmore IR, Fox SP, Hollins AJ, Sohail M, & Akhtar S (2004) The design and exogenous delivery of siRNA for post-transcriptional gene silencing. *J Drug Target* 12(6):315-340.
19. Kong D, *et al.* (2005) Echinomycin, a small-molecule inhibitor of hypoxia-inducible factor-1 DNA-binding activity. *Cancer Res.* 65(19):9047-9055.
20. Nickols NG, Jacobs CS, Farkas ME, & Dervan PB (2007) Modulating hypoxia-inducible transcription by disrupting the HIF-1-DNA interface. *Acs Chemical Biology* 2(8):561-571.

21. Cheng JC, Moore TB, & Sakamoto KM (2003) RNA interference and human disease. *Mol Genet Metab* 80(1-2):121-128.
22. Edelson BS, *et al.* (2004) Influence of structural variation on nuclear localization of DNA-binding polyamide-fluorophore conjugates. *Nucleic Acids Res* 32(9):2802-2818.
23. Dervan PB & Edelson BS (2003) Recognition of the DNA minor groove by pyrrole-imidazole polyamides. *Curr Opin Struct Biol* 13(3):284-299.
24. Nickols NG & Dervan PB (2007) Suppression of androgen receptor-mediated gene expression by a sequence-specific DNA-binding polyamide. *Proc. Natl. Acad. Sci. U. S. A.* 104(25):10418-10423.
25. Muzikar KA, Nickols NG, & Dervan PB (2009) Repression of DNA-binding dependent glucocorticoid receptor-mediated gene expression. *Proc. Natl. Acad. Sci. U. S. A.* 106(39):16598-16603.
26. Raskatov JA, *et al.* (2012) Modulation of NF-kappaB-dependent gene transcription using programmable DNA minor groove binders. *Proc. Natl. Acad. Sci. U. S. A.* 109(4):1023-1028.
27. Matsuda H, *et al.* (2006) Development of gene silencing pyrrole-imidazole polyamide targeting the TGF-beta1 promoter for treatment of progressive renal diseases. *J Am Soc Nephrol* 17(2):422-432.
28. Yang F, *et al.* (2013) Antitumor activity of a pyrrole-imidazole polyamide. *Proc. Natl. Acad. Sci. U. S. A.* 110(5):1863-1868.
29. Synold TW, *et al.* (2012) Single-dose pharmacokinetic and toxicity analysis of pyrrole-imidazole polyamides in mice. *Cancer Chemother. Pharmacol.* 70(4):617-625.
30. Raskatov JA, *et al.* (2012) Gene expression changes in a tumor xenograft by a pyrrole-imidazole polyamide. *Proc. Natl. Acad. Sci. U. S. A.* 109(40):16041-16045.
31. Kashiwazaki G, *et al.* (2012) Synthesis and biological properties of highly sequence-specific-alkylating N-methylpyrrole-N-methylimidazole polyamide conjugates. *J Med Chem* 55(5):2057-2066.
32. Wang X, *et al.* (2010) Inhibition of MMP-9 transcription and suppression of tumor metastasis by pyrrole-imidazole polyamide. *Cancer Sci* 101(3):759-766.
33. Olenyuk BZ, *et al.* (2004) Inhibition of vascular endothelial growth factor with a sequence-specific hypoxia response element antagonist. *Proc. Natl. Acad. Sci. U. S. A.* 101(48):16768-16773.
34. Vacca A, *et al.* (1994) Bone marrow angiogenesis and progression in multiple myeloma. *Br J Haematol* 87(3):503-508.
35. Vacca A, *et al.* (1995) Bone marrow of patients with active multiple myeloma: angiogenesis and plasma cell adhesion molecules LFA-1, VLA-4, LAM-1, and CD44. *Am J Hematol* 50(1):9-14.
36. Rajkumar SV, *et al.* (2000) Prognostic value of bone marrow angiogenesis in multiple myeloma. *Clin Cancer Res* 6(8):3111-3116.
37. Kumar S, *et al.* (2004) Effect of thalidomide therapy on bone marrow angiogenesis in multiple myeloma. *Leukemia* 18(3):624-627.
38. White D, *et al.* (2013) Results from AMBER, a randomized phase 2 study of bevacizumab and bortezomib versus bortezomib in relapsed or refractory multiple myeloma. *Cancer* 119(2):339-347.
39. Blagosklonny MV (2004) Antiangiogenic therapy and tumor progression. *Cancer Cell* 5(1):13-17.

40. Warfel NA & El-Deiry WS (2014) HIF-1 signaling in drug resistance to chemotherapy. *Curr Med Chem* 21(26):3021-3028.
41. Hu J, et al. (2013) Synergistic induction of apoptosis in multiple myeloma cells by bortezomib and hypoxia-activated prodrug TH-302, in vivo and in vitro. *Mol Cancer Ther* 12(9):1763-1773.
42. Billadeau D, et al. (1997) Activating mutations in the N- and K-ras oncogenes differentially affect the growth properties of the IL-6-dependent myeloma cell line ANBL6. *Cancer Res* 57(11):2268-2275.
43. Chun SY, et al. (2010) Oncogenic KRAS modulates mitochondrial metabolism in human colon cancer cells by inducing HIF-1alpha and HIF-2alpha target genes. *Mol Cancer* 9:293.
44. Hoang B, et al. (2006) Oncogenic RAS mutations in myeloma cells selectively induce cox-2 expression, which participates in enhanced adhesion to fibronectin and chemoresistance. *Blood* 107(11):4484-4490.
45. Frost P, Shi Y, Hoang B, Gera J, & Lichtenstein A (2009) Regulation of D-cyclin translation inhibition in myeloma cells treated with mammalian target of rapamycin inhibitors: rationale for combined treatment with extracellular signal-regulated kinase inhibitors and rapamycin. *Mol Cancer Ther* 8(1):83-93.
46. Ahmadi M, et al. (2014) Hypoxia modulates the activity of a series of clinically approved tyrosine kinase inhibitors. *British journal of pharmacology* 171(1):224-236.
47. Frost P, et al. (2004) In vivo antitumor effects of the mTOR inhibitor CCI-779 against human multiple myeloma cells in a xenograft model. *Blood* 104(13):4181-4187.
48. Frost P, Shi Y, Hoang B, & Lichtenstein A (2007) AKT activity regulates the ability of mTOR inhibitors to prevent angiogenesis and VEGF expression in multiple myeloma cells. *Oncogene* 26:2255-2262.
49. Frost P, et al. (2013) Mammalian target of rapamycin inhibitors induce tumor cell apoptosis in vivo primarily by inhibiting VEGF expression and angiogenesis. *J Oncol* 2013:897025.
50. Miyakawa Y, et al. (2004) Establishment of a new model of human multiple myeloma using NOD/SCID/gammac(null) (NOG) mice. *Biochem Biophys Res Commun* 313(2):258-262.
51. Dewan MZ, et al. (2004) Prompt tumor formation and maintenance of constitutive NF-kappaB activity of multiple myeloma cells in NOD/SCID/gammacnull mice. *Cancer Sci* 95(7):564-568.
52. Shi Y, et al. (2002) Enhanced sensitivity of multiple myeloma cells containing PTEN mutations to CCI-779. *Cancer Res* 62(17):5027-5034.
53. Brugarolas J, et al. (2004) Regulation of mTOR function in response to hypoxia by REDD1 and the TSC1/TSC2 tumor suppressor complex. *Genes Dev.* 18(23):2893-2904.
54. Vadysirisack DD & Ellisen LW (2012) mTOR activity under hypoxia. *Methods Mol. Biol.* 821:45-58.
55. Semenza GL (2013) HIF-1 mediates metabolic responses to intratumoral hypoxia and oncogenic mutations. *J. Clin. Invest.* 123(9):3664-3671.
56. Hoang B, Benavides A, Shi Y, Frost P, & Lichtenstein A (2009) Effect of autophagy on multiple myeloma cell viability. *Mol Cancer Ther* 8(7):1974-1984.
57. Shi Y, et al. (2011) IL-6-induced enhancement of c-myc translation in multiple myeloma cells: critical role of cytoplasmic localization of the RNA-binding protein hnRNP A1. *J Biol Chem* 286(1):67-78.

58. Shi Y, *et al.* (2013) MNK kinases facilitate c-myc IRES activity in rapamycin-treated multiple myeloma cells. *Oncogene* 32(2):190-197.
59. Arsham AM, Howell JJ, & Simon MC (2003) A novel hypoxia-inducible factor-independent hypoxic response regulating mammalian target of rapamycin and its targets. *J Biol Chem* 278(32):29655-29660.
60. Sofer A, Lei K, Johannessen CM, & Ellisen LW (2005) Regulation of mTOR and cell growth in response to energy stress by REDD1. *Mol Cell Biol* 25(14):5834-5845.
61. Braunstein S, *et al.* (2007) A hypoxia-controlled cap-dependent to cap-independent translation switch in breast cancer. *Mol Cell* 28(3):501-512.
62. Stein I, *et al.* (1998) Translation of vascular endothelial growth factor mRNA by internal ribosome entry: implications for translation under hypoxia. *Mol Cell Biol* 18(6):3112-3119.
63. Hoang B, *et al.* (2012) The PP242 mammalian target of rapamycin (mTOR) inhibitor activates extracellular signal-regulated kinase (ERK) in multiple myeloma cells via a target of rapamycin complex 1 (TORC1)/eukaryotic translation initiation factor 4E (eIF-4E)/RAF pathway and activation is a mechanism of resistance. *J Biol Chem* 287(26):21796-21805.